Science of the Total Environment 712 (2020) 136513

Contents lists available at ScienceDirect

Science of the Total Environment

journal homepage: www.elsevier.com/locate/scitotenv

Autochthonous N-doped carbon nanotube/activated carbon composites derived from industrial paper sludge for chromate (VI) reduction in microbial fuel cells

Shaofeng Zhou [a], Beiping Zhang [a], Zhiyang Liao [a], Lihua Zhou [b], Yong Yuan [a,*]

[a] Guangzhou Key Laboratory Environmental Catalysis and Pollution Control, Guangdong Key Laboratory of Environmental Catalysis and Health Risk Control, School of Environmental Science and Engineering, Institute of Environmental Health and Pollution Control, Guangdong University of Technology, Guangzhou 510006, China
[b] Institute of Natural Medicine & Green Chemistry, School of Chemical Engineering and Light Industry, Guangdong University of Technology, Guangzhou 510006, China

HIGHLIGHTS

- N-doped CNT/AC composites was evolved from industrial paper sludge waste.
- Melamine played a key role on carbon nanotubes growth.
- The carbon nanocomposites exhibited fascinating electroactivity.
- Cr(VI) removal performance of MFC linked with biochar's electroactivity.

GRAPHICAL ABSTRACT

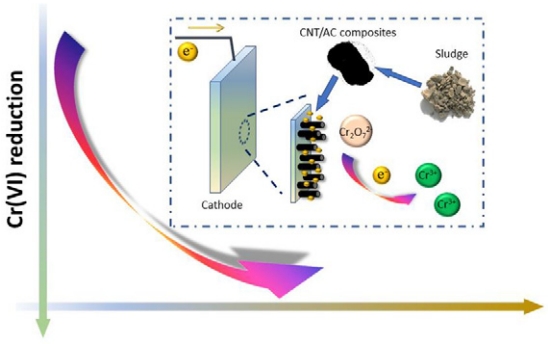

ARTICLE INFO

Article history:
Received 6 November 2019
Received in revised form 19 December 2019
Accepted 2 January 2020
Available online 7 January 2020

Editor: Yifeng Zhang

Keywords:
Biochar
Industrial paper sludge
Carbon nanotubes
Microbial fuel cell
Chromate reduction

ABSTRACT

The performance of microbial electrochemical system for hexavalent chromium (Cr(VI)) contaminant has been a severe challenge remaining active for further development. In this study, we developed a novel biochar material from industrial paper sludge for microbial fuel cell cathode fabrication to reduce aquatic Cr(VI) to non-toxic Cr (III). With additive melamine as nitrogen source and self-containing small portion of Fe as catalyst, the sludge evolved into electroactive biochar (BC-M) rendering a unique N-doped carbon nanotubes/activated carbon (N-CNT/AC) frame after pyrolyzed at 900 °C for 2 h. Electrochemical analysis revealed enhanced electron transference capacity of this composite material, such effectiveness was attributed to the increased surface area and superior electroconductivity of N-doped CNTs. For performance of Cr(VI) reduction, a 55.1% reduction efficiency was achieved in an microbial fuel cell equipped with BC-M cathode while it reduced to about 41.8% when the cathode was replaced by electrode modified with no-melamine-involved biochar. The strategy of biochar upgrading from industrial paper sludge proposed in this work is expected to not only bring technical solution for low-cost CNT materials preparation for Cr(VI) reduction, but also put forward further research on value-added chemical synthesis from waste in various fields of energy and environment.

* Corresponding author.
E-mail address: yuanyong@soil.gd.cn (Y. Yuan).

https://doi.org/10.1016/j.scitotenv.2020.136513
0048-9697/

1. Introduction

Microbial electrochemical system (MES) recently has been regarded as a green and sustainable alternative biotechnology for heavy metal removal/recovery as it holds great advantages like energy-efficient (Zhang and Angelidaki, 2014). In MES, electrons could be delivered from anode to cathode where heavy metals could act as an oxidant to close the circuit for electric energy output. Mainstream research in last decade provides an abundant collection of literature on this field, ranging from copper recovery to divalent cadmium (Cd^{2+}) reduction. Among these, the reduction of hexavalent chromium (Cr(VI)) in MES is attracted prior attentions worldwide since Cr(VI) may cause irreversible environmental adversity and severe human diseases like cancer through its chronic exposure and bio-accumulation (Bharath et al., 2019; Bharath et al., 2020; Bibi et al., 2018; Lei et al., 2018). The detoxication is based on the reduction from chromate to trivalent chromium (Cr(III)) that is considered relatively less ecotoxic due to weak mobility (Eq. (1)) (Hsu et al., 2012; Kim and Choi, 2011; Li and Zhou, 2019; Li et al., 2019; Wang et al., 2017).

$$CrO_4^{2-} + 7H^+ + 3e_{aq}^- \rightarrow Cr^{3+} + 4H_2O \quad (1)$$

Previous works have demonstrated the reduction capacities of biocathode in MES (Tandukar et al., 2009; Xafenias et al., 2013). In these cases, electroactive biofilms attached on cathode are running as biocatalysts to drive chromate reduction. But the microbial consortia could be potentially poisoned by Cr(VI) as well thus efficiency would decrease over time (Zhang et al., 2019b). Besides, it is intractable for cultivating the biofilms on cathode with satisfying and stable amount of biomass in acidic condition (pH < 4) which is beneficial to chromate reduction. Thus, researchers turned eyes toward traditional microbial fuel cell architecture assembled with abiotic cathode, merging the advantages of bioenergy and chemical efficiency (Li et al., 2018; Zhang et al., 2019c). Since the reduction of Cr(VI) to lower oxidation state (Cr(III)) highly replies on indigenous infrastructure and subsequent electron-transfer capability of electrode surface, cathode decorated with some certain redox-activated catalysts have populated among literatures. For instance, S. Gupta et al. demonstrated an innovative alumina-nickel nanoparticles-dispersed carbon nanofiber electrode for Cr(VI) reduction which achieved columbic efficiency of 93% with a complete removal of Cr(VI) (Gupta et al., 2017). In this case, the transition metal, nickel (Ni), made a crucial contribution in electron transfer for Cr(VI) removal (Gupta et al., 2017). Though promising, still, scientific community is looking for a catalyst in a more recyclable and sustainable way.

Wastewater/industrial sludge as a resource for conversion into useful biochar chemicals has been a hotpot of trash-to-treasure concept (Zhou et al., 2019). Biochar derived from various sludge has been upgraded to activators for advanced oxidation process, adsorbents for oil pollutants and widely applied into various environmental areas (Qian et al., 2019; Tao et al., 2019; Wang et al., 2019). For example, Wang et al. highlighted the fast activation of peroxymonosulfate in triclosan-containing wastewater remediation in the presence of sludge-derived biochar, achieving total organic carbon removal rate of 32.5% within 240 min-operation (Wang and Wang, 2019). More than that, of particular interest is the electrochemical properties of these biochar, that is, directly introduces biochar into redox-oriented reactions with pollutants (Zhang et al., 2019d; Zhong et al., 2019). Theoretically, the sludge is carbon-abundant mixture that may contribute to sludge upgrading to carbonaceous redox-active catalysts during facile thermal treatments (Yuan et al., 2017). With Aeschbacher et al., 2010 this potential, environmental implications of sludge-derived biochar should be further explored based on its excellent redox capacity. In this regard, it is possible to fabricate cathode of MFC with sludge-derived biochar catalysts for chromate reduction. However, to date no relevant research has ever been reported.

Herein, for the first time we provided a facile strategy for redox-active biochar material derived from industrial paper sludge. The morphology, electrochemical activity and underlying mechanisms of such biochar materials were analyzed. The carbonaceous material was then employed to fabricate cathode of microbial fuel cells for hexavalent chromium reduction. The outcomes are expected to offer an efficient and sustainable protocol that merges the advantages of sludge re-utilization and microbial electrochemical system for detoxification of heavy metals.

2. Materials and methods

2.1. Preparation of biochar materials

The biochar was synthesized from industrial paper sludge following a facile pyrolysis process (Fig. S1). Briefly, the sludge (collected from wastewater treatment of NG Paper Industry Ltd. Co., Dongguan, China) was naturally air-dried for several days and further grinded manually to pass through a 100-mesh sieve. After this pretreatment, the powders were then fully mixed with melamine powder at a mass ratio of 1:1 as our pre-experiments found this ratio was optimal for carbon nanotubes generation. The pyrolysis procedure was programmed to increase to 900 °C from ambient temperature with a heating rate of 5 °C min^{-1} and maintained at 900 °C for 2 h under a pure nitrogen atmosphere. Samples were subsequently soaked and stirred in 0.5 M HCl for 3 h and thoroughly washed by deionized water several times till neutral pH. The as-prepared carbon composites were finally collected after drying at 45 °C for 12 h and denoted as BC-M. Another biochar samples were also obtained following the same procedure but without melamine for comparison (denoted as BC).

2.2. Reactors operation and cathodes fabrication

A conventional H-type dual-chamber MFC reactor modified from reagent bottles was employed in this study. The anode and cathode chambers had an equal effective volume of 120 mL and they were separated by a proton exchange membrane (Nafion 117, Dupont Co., USA.). In the enrichment stage of MFC, a carbon brush (3 cm in diameter, 3 cm in length, Mill- Rose, USA) and a plain graphite plate (3 cm × 3 cm × 0.4 cm) were installed as anode and cathode, respectively, connected by titanium wires via an external resistance (ER) of 1000 Ω. Anaerobic sludge (Liede municipal wastewater treatment plant, Guangzhou, China) amended by 1 g/L acetate was added into anode chamber as inoculum. After two-week start-up, nutrient solution was added into anode chamber instead of anaerobic sludge. The components of nutrient solution for anodic electricigens cultivation and detailed enrichment procedure were described in previous publications (Zhou et al., 2018a; Zhou et al., 2018b). When the maximum electricity output of MFC reproducibly reached ~650 mV in consecutive batches, the mature anodic biofilm was recognized well-formed and stabilized.

Prior to electrode coating, several graphite plates were successively soaked and cleaned in acetone, ethanol and deionized water to removal surface impurities. 100 mg biochar materials were severely mixed with 200 μL absolute ethanol and 10 μL Nafion solution (5%, DuPont Co., USA) to form a homogeneous suspension. This biochar-contained suspension was then uniformly spread onto clean graphite plate using a fuzz brush, followed by air-dried for 12 h.

Table 1
The respective elemental compositions of biochar specimen derived from sludge biomass.

Samples	Elemental content %				
	C	O	N	Fe	S
BC-M	84.94	7.64	6.36	0.68	0.38
BC	73.00	24.04	1.6	0.74	0.62

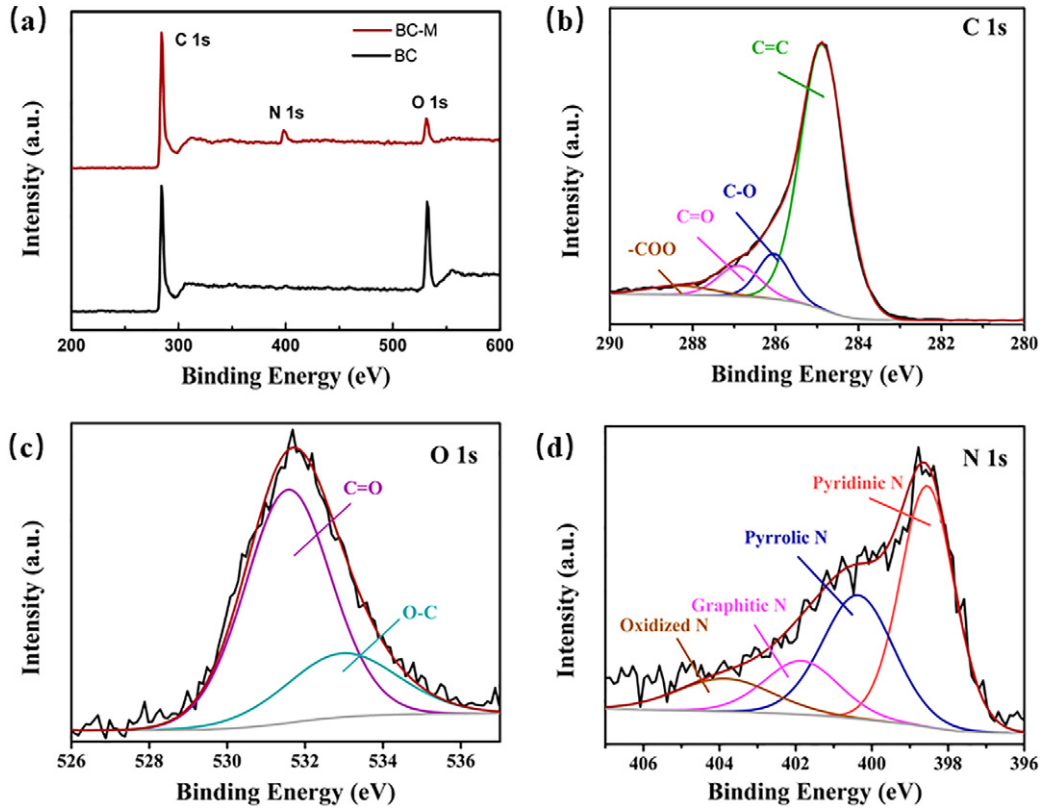

Fig. 1. (a) Full scan XPS spectra of biochar samples and high-resolution C 1s (b), O 1s (c), and N 1s (d) XPS spectra of BC-M composites.

For Cr (VI) reduction tests, the cathode was substituted by biochar modified electrode while the external resistance was switched to 100 Ω. Subsequently. the catholyte was replaced by 50 mM Na_2SO_4 solution containing 20 mg (Cr(VI))/L except otherwise stated. The initial pH of catholyte was adjusted to 3.0 by 0.1 M H_2SO_4 before each test. Both chambers were covered by aluminum foil to exclude light and flashed with nitrogen gas for at least 15 min before every batch. Samples were taken out at pre-determined intervals. All experiments were conducted triplicate at ambient temperature (35 °C).

2.3. Electrochemical analysis

The voltage of MFC across the external resistance was on-line recorded by a digital multimeter (Model 2700, Keithley Instrument Co., USA). For tests of cyclic voltammetry (CV) and linear sweep voltammetry (LSV), 10 μL of the carbon components-Nafion suspension was spiked onto a glassy carbon rotating disk electrode (7 mm^2, OrigaTrod, France). Prior to use, the plain electrode was orderly polished by Al_2O_3 powder (0.3 μm and 0.05 μm in size), and then cleaned by deionized

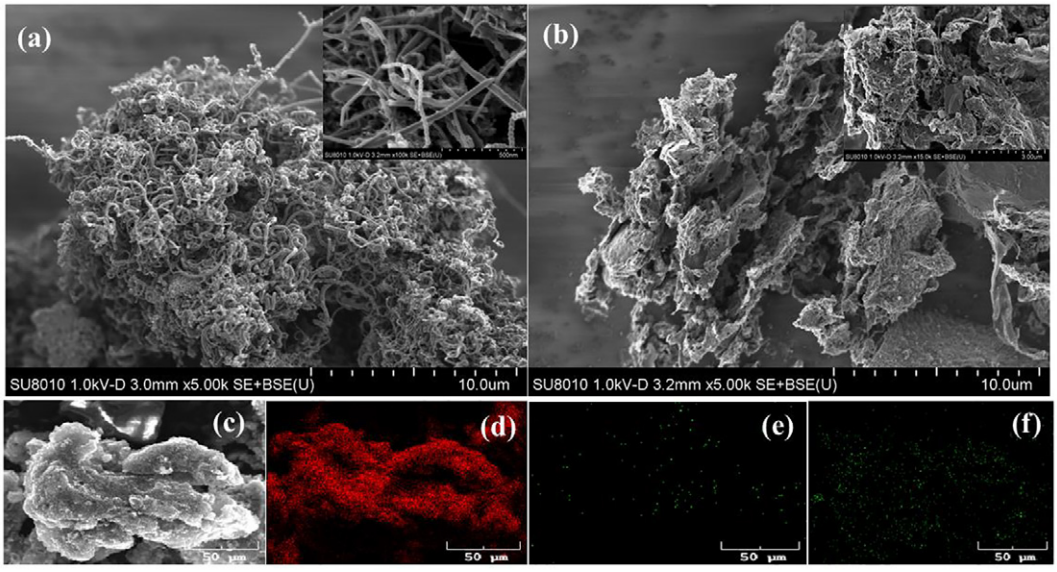

Fig. 2. SEM images of BC-M ((a) and (c)) and BC (b) materials with or without melamine (Insert: larger magnification), Elemental mappings of BC-M for (d) C, (e) N and (f) Fe.

water. A platinum plate (1 × 1 cm) and an Ag/AgCl electrode (+0.197 V, all potentials presented in this article versus this reference) were set as counter electrode and reference electrode, respectively. Notably, all CV and LSV tests were all conducted under anaerobic condition as well.

To further qualify the electron transfer capacity (ETC) of biochar, the electron donating capacity (EDC) and electron accepting capacity (EAC) of as-prepared biochar were investigated in this study, following a typical mediated electrochemical reduction (MER) and oxidation (MEO) process (Aeschbacher et al., 2010). These tests were anaerobically carried out in a three-electrode system similar with CV test except that a glassy-carbon-made cylinder with a working volume of 15 mL was employed for both reaction vessel and working electrode. The vessel was filled with 0.1 M KCl as electrolyte and constant potentials (i.e., $E_h = -0.49$ V for MER and $E_h = 0.61$ V for MEO, respectively) were applied. Prior to each test, diquat dibromide (DQ) and 2,2′-Azino-bis(3-ethylbenzthiazoline-6-sulfonic acid) (ABTS) were injected into the vessel as extraneous mediators for MER and MEO, respectively (Zhang et al., 2019a). System current intensity was continuously recorded and gradient increasing amounts of biochar (0.08 mg to 0.4 mg) were spiked into the reactor when system current stabilized. The values of EAC and EDC were calculated following the eqs. (2) and (3) (Zhang et al., 2019a):

$$\mathrm{EAC} = \cdot \int \frac{\frac{I_{red}}{F} dt}{m} \tag{2}$$

$$\mathrm{EDC} = \cdot \int \frac{\frac{I_{ox}}{F} dt}{m} \tag{3}$$

where I_{red} and I_{ox} are reductive and oxidative currents recorded in MER and MEO process, respectively. F presents Faraday constant as 96,485 (C/mol) while m [g biochar] stands for the dosage amounts of biochar. ETC was calculated as the sum of EAC and EDC. Experiments were conducted at least duplicate and the stabilization of electric current as baseline for separation of individual current peaks was ensured before each biochar dosage.

2.4. Materials characterization

The surface structure and elements distribution of specimen were examined by field scanning electron microscope (SEM) with energy dispersive X-ray spectroscopy (EDS) (SU8010, Hitach, Japan) and transmission electron microscopy (TEM) (F200S, FEI Thermo, Czech). For Raman test, samples were illuminated at a wavelength of 633 nm (inVia Reflex, Renishaw, UK). The specific surface area of different composites was calculated via Brunauer-Emmett-Teller (BET) method (Micromeritics ASAP 2020 adsorption analyzer, USA). The elements composition analysis was conducted based on the results of X-ray photoelectron spectroscopy (XPS) (ESCALAB-250, Thermo Fisher Scientific, USA). The Cr(VI) concentration was detected via colorimetric method at a wavelength of 540 nm by UV–Vis spectrophotometer (UV-2600, Shimadzu, Japan) (Li et al., 2018). The samples were also analyzed by an X-ray diffractometer (XRD) (Xpert Powder, Panalytical, Nertherland).

3. Results and discussions

3.1. Characterization of the as-prepared biochar

As elucidated via XPS analysis, the presence of C, O, N and Fe were confirmed in all biochar samples (Table 1 and Fig. 1 & S2). Among them, three predominant peaks were located at 284.6 eV, 401.0 eV and 531.2 eV for C 1 s, N 1 s and O 1 s, respectively (Fig. 1a). Although limited difference on C 1 s and O 1 s of two biochar samples was observed (Fig. S2), noteworthy, the N intensity in XPS of BC was much lower than that of BC-M which was pyrolyzed in the presence of melamine (Fig. S2 and Table 1), this suggested that nitrogen was successfully doped in these BC-M materials. It also should be noted that only a few Fe element had been detected via XPS in all samples as it might be flushed away during acidic washing. Relevant details on elements compositions and chemistry of as-prepared carbonaceous materials (BC-M) are

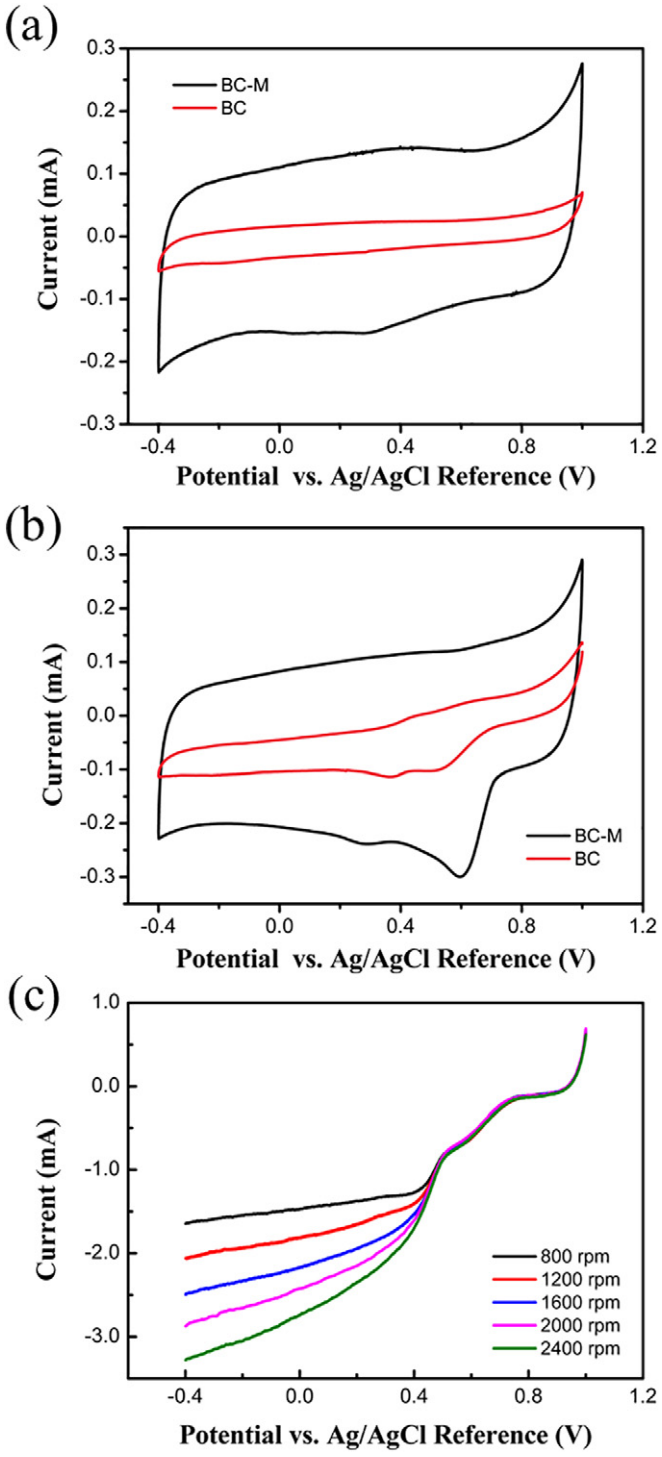

Fig. 3. (a) Typical CV curves of biochar-fabricated working electrodes. (Electrolyte base: 0.1 M HCl, Scan rate: 10 mV/s), (b) CV and (c) LSV curves of BC-M in 0.1 M HCl solution containing 0.14 g(Cr(VI))/L, scan rate: 10 mV/s, (d) simplified scheme of electrochemical reduction of Cr(VI). (GC: pristine glassy carbon electrode).

shown in Fig. 1. First of all, the high resolution of C 1s spectrum displayed four major components related to C—C/C═C bond of the sp^2 graphitic carbon (284.5 eV), C—O bond (285.5 eV), C═O bond (286.7 eV) and O—C═O bond (288.9 eV), respectively (Zhou et al., 2017). Similarly, for O 1s spectrum, it was found to entail two distinguishable oxygen moieties. These fitted peaks at 532.4 and 534.6 eV was assigned to oxygen-containing functional groups (C—O and C═O, respectively) (Liang et al., 2014). Besides, N peaks of BC sample were hardly resolved from the high-resolution N 1s spectra (Fig. S2), while that of BC-M was resolved to four peaks at binding energy of 404.1 eV, 401.7 eV, 400.3 eV and 397.7 eV, assigned to oxidized, graphitic, pyrrolic and pyridinic N, respectively (Zhou et al., 2016). In consequence, the XPS results clearly highlighted the multi-forms of N in BC-M materials and oxygen-containing functional groups which were of significance for redox-oriented reactions. As for Raman spectra, two characteristic peaks (D-band and G-band) were detected at 1350 and 1600 cm^{-1}, respectively (Fig. S3a). This results clearly presented a graphitized carbon forms in nanocomposites. A quite low intensity ratio ($I_D/I_G < 1.0$) further proved the graphitization of biochar (Gupta et al., 2017). Relevant discussions were accordingly added in manuscript. The XRD analysis provided information of graphitization degree of different samples (Fig. S3b). The series of peaks observed in Precursor clearly indicated various inorganic components in sludge powder. After pyrolysis, the significant increase in intensity of (002) peak at 26° of biochar samples evidenced a good graphitic degree during carbonization.

Comparative materials were synthesized following similar procedure to identify vital factors involving in the formation of structure and morphology. The morphologies and EDS profiles of the prepared materials were presented in Fig. 2. The geometric feature with agglomerated and curly forms of carbon nanotubes at an average transection diameter of 50 nm could be clearly recognized in BC-M. The unique carbon nanotubes structure was also evidenced by TEM (Fig. S4). On the other hand, no interwinding CNTs but a dense carbon monolith was obtained without the addition of melamine (Fig. 2a and b). Such observation indicated that after thermal treatment (900 °C), sludge powders could be further upgraded to N-doped carbon nanotubes/activated carbon (N-CNT/AC) in the presence of melamine. Such evolution could be divided into two stages. Part of sludge powder was firstly carbonized under hyperthermal condition, transforming into a mesoporous carbon cadre as suitable base for the carbon nanotube growth (Li et al., 2017). As the sludge used in this study contained a small amounts of Fe (shown in Table 1 and elementary mapping in Fig. 2f), it was able to progressively auto-catalyze gasified moieties of sludge powders, together with gasified melamine molecules as key source for heteroaromatic nitrogen doping and nanotubes formation, into a unique three-dimensional nitrogen-doped carbon nanomaterials layer by layer (Chen et al., 2019; Li et al., 2017).

3.2. Electrochemical analysis

The electrochemical properties of as-synthesized biochar materials were evaluated via CV and LSV in N_2-saturated condition. Typical and reproducible curves were presented in Fig. 3. It could be seen that the recorded currents of BC-M modified electrode significantly outpaced that of no-melamine-involved biochar (Fig. 3a). The enhancement could be ascribed to the micro-morphological three-dimensional cadre of BC-M, which provided abundant active sites and larger superior surface area. As for Cr(VI) electrochemical reduction, a reduction peak at ~0.6 V was detected in the CV curves (Fig. 3b). This could be identified as occurrence of Cr(VI) reduction catalyzed by biochar modified electrode. Furthermore, it is worth noting that the BC-M not only amplified the current of reduction peak but slightly brought a more positive onset of reduction. These results confirmed the feasibility of BC-M as an efficient electrode modifier for chromate reduction. Furthermore, Fig. 3c shows the linear sweep voltammogram profiles of BC-M coated electrode at various rotating speeds. Apparently, gradient increase currents with onset at 0.5–0.6 V were recorded with an increase of rotating speeds, indicating a close correlation between the amounts of transferred electrons and Cr(VI) reduction process. It could be deduced that the Cr(VI) electrochemical reduction was mainly controlled by mass transfer rather than electrochemical performance of BC-M, which, in turn, further confirmed the catalytic property of BC-M.

The applicability of electrons mediating capability was also evaluated to quantitatively reinforce electrochemical properties of BC-M. Fig. 4a presents baseline-corrected current-time response curves with successive dosages of biochar samples. The results support a clear linearly proportional relationship between the electron accepting or donating capacity (Q) and adding amounts of biochar. The vales of EDC and EAC, calculated based on Eqs. (2) & (3), were 0.0229 and 0.284 $mmol_{e^-}/g$ biochar for BC-M, respectively, which were ~29.3% and ~62.2% higher than that of BC, respectively (Fig. 4b). This means that there is a strong connection between the electron transference capacity and heteroaromatic nitrogen doping.

Comprehensively, the formation of carbon nanotubes/activated carbon brought superb electrochemical activity to the new materials. The introduction of nitrogen element in forms of pyridinic-N and graphitic-N into the upgrading process from sludge biomass to N-CNT/AC composites could be critically instrumental for unique electrochemical features (Sharma et al., 2015). For example, it is widely considered that nitrogen in pyridine-like structure accumulates excess negative charge around N atoms, resulting in high-level Faradic reaction-based properties (Lei et al., 2018). Similar to pyridinic nitrogen, the graphitic-N located electrons in the π* antibonding orbital, still responsible for lowering overpotential for the case of reduction reactions, compared to the pristine CNTs (Sharma et al., 2015). From another point of view, a growth of graphitized carbon matrix was achieved at high

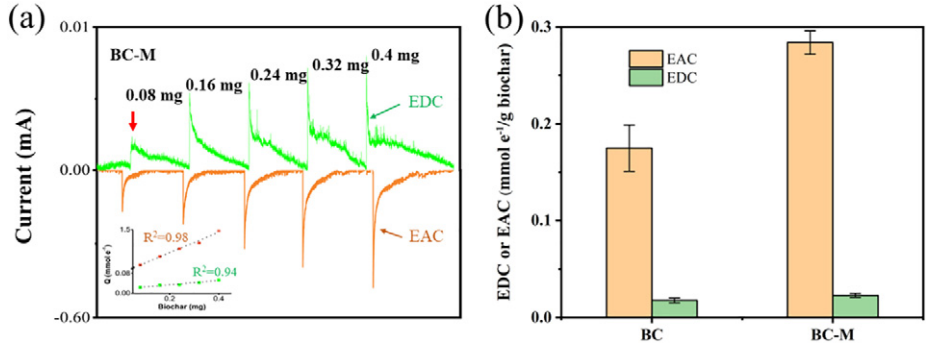

Fig. 4. (a) Oxidative and reductive current responses of BC-M (Insert: Linear relationship between transferred electron amounts and gradient increasing dosages of BC-M), (b) electron transfer capacity of BC and BC-M.

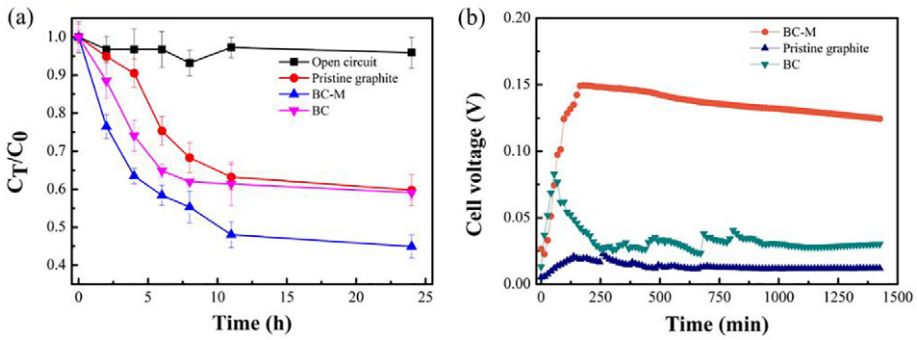

Fig. 5. (a) Cr(VI) reduction performance of different biochar and blank control, (b) Profiles of cell voltage of different MFC configurations (ER = 100 Ω, catholyte: 20 mg (Cr(VI))/L in 50 mM KCl solution, initial pH = 3.0).

pyrolysis temperature (900 °C in this case) which enhanced conductivity of the carbon materials (Yuan et al., 2017). Furthermore, the upgrading from biochar (BC) to N-CNT/AC composites (BC-M) led to an increase of 41.8% in BET surface area from 140.85 m^2/g to 199.05 m^2/g. This increase renovated porosity of BC-M that allowed exoteric redox reactants easily reach the active moieties in biochar (Yuan et al., 2017). Thus, the catalytic activity of such materials could be significantly boosted by merging the advantages.

3.3. Cr(VI) reduction performance

The BC-M electrodes were assembled in a typical microbial fuel cell to examine feasibility of its catalytic property for hexavalent chromium reduction and the results are shown in Fig. 5. As acidification of solution might lead to higher Cr(VI) reduction efficiency (Fig. S5), an initial pH of ~3.0 was chosen in this study to provide sufficient protons for Cr(VI) reduction as shown in Eq. (1). For BC-M group, the concentrations of Cr (VI) dramatically decreased from initial ~20 mg/L to approximately 9 mg/L, achieving a 55% reduction rate in 24 h (Fig. 5a). The reduction of Cr(VI) presented a pseudo-first-order kinetic in the first 11 h, followed by a much slower rate of Cr(VI) reduction subsequently. Comparatively, such reduction process was much weakened in the absence of biochar fabrication. <40% Cr(VI) was reduced during identical reaction time. Interestingly, those cathodes that coated with non-melamine modified biochar also presented poor Cr(VI) removal efficiency (40%), nearly maintaining at the level of that of pristine graphite. It was worth noting that very limited Cr(VI) reduction (< 5%) was detected in open-circuit group in which cathode and anode were disconnected. It indicated that physical absorption of as-prepared biochar materials could be negligible, confirming that major Cr(VI) was removed via redox-oriented reactions in this system. This was very important because detoxification of the heavy metal relies on conversion lower-valent state over physical absorption (Han et al., 2018). An additional evidence was presented in Fig. 5b. The energy output of MFC with BC-M modified cathode was highest and relatively stable during full operation time, since N-defect sites inside the N-CNT/AC composites were expected to promote the proton-electron pair transfers (Sharma et al., 2015). On the other hand, there was only a limited enhancement in recorded voltage of MFC with BC modified cathode compared with that of MFC assembled with pristine graphite as cathode, indicating the AC composites had little to do within the electricity output of the system. The results showed the importance of CNT/AC composites in biochar to the promoted electron transfer efficiency of MFC. Except for the superb electrochemical properties of BC-M, another contribution for this promotion was also on account of nitrogen doping which endowed plentiful active sites at the edge and surface of the carbon matrix, facilitating mass adsorption and transport (Chen et al., 2019).

A comparison based on Cr(VI) removal of MFCs proposed from existing literature was made (Table 2). Since the concept of reducing Cr(VI) by MFC was proposed (Tandukar et al., 2009), the scientific community has witnessed an impressive progress on both Cr(VI) removal efficiency and power density, with the modification of cathode or addition of electron shuttles. The comparative information clearly indicates that the Cr(VI) removal efficiency of this study was superior to some of other studies. Although a higher removal efficiency of 75% was achieved by Pang et al. by employing a couple of highly-active electron exchange agents (PPy/AQS) (Pang et al., 2013), this study presented a slight advantage on current density.

In order to further investigate the surface transformation of BC-M in long-term operation. The BC-M modified cathode was subsequently examined by SEM after five consecutive operations and results are shown in Fig. 6. It could be noted that a chromium deposition was detected in large amounts on the surface of cathode. As discussed above, Cr(VI) was barely observed onto the electrode, thus this precipitation during Cr(VI) reduction process was largely composed of Cr(III) in the form

Table 2
Comparison of studies of hexavalent chromium removal performance in MFCs.

No.	Cathode materials	Initial Cr(VI) concentration (mg/L)	Working volume (mL)	Removal efficiency	Current density (mA/m^2)	Reference
1	Biofilm on graphite plate	60	–	100% in 6 d	123.4	(Tandukar et al., 2009)
2	PPy/AQS modified graphite felt	20	100	~75% in 24 h	~1100	(Pang et al., 2013)
3	Alumina-nickel modified carbon nanofiber	100	200	~50% in 24 h	4560	(Gupta et al., 2017)
4	Carbon cloth	50	350	~50% in 8 h with addition of 50 mg/L Cu (II)	–	(Li and Zhou, 2019)
5	Carbon cloth	80	340	~25% in 24 h and 100% in 120 h	–	(Li et al., 2018)
6	N-CNT/AC modified graphite	20	100	55.1% in 24 h	1666.6	This study

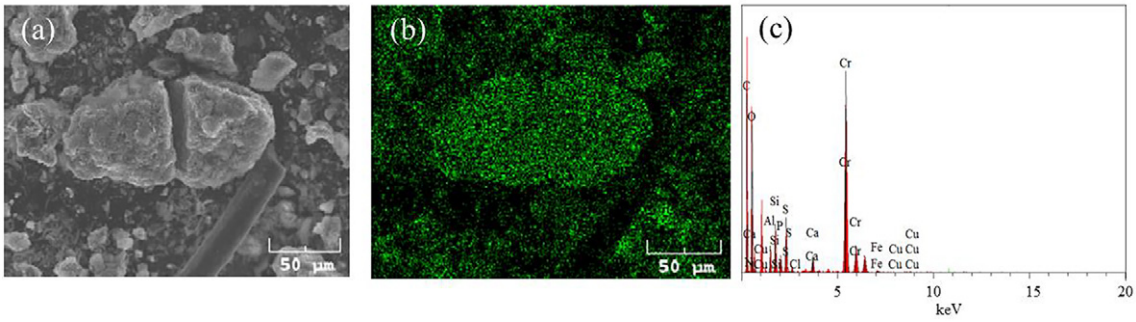

Fig. 6. (a) SEM images, (b) elemental mapping of Cr and (c) EDS spectrum of BC-M coated graphite plate after Cr(VI) reduction. Samples were taken out of MFC after five consecutive operation.

of $Cr(OH)_3$ with continuing increased catholyte pH (from 3.0 to above 9.5) (Chen et al., 2015; Xafenias et al., 2013). Although the precipitation may to some extent slightly decreased service life of cathode, this issue could be easily solved by acid cleaning of cathode, enlarging working volume of cathode chamber or addition of suitable base. Nevertheless, this study presents an sustainable evolution from waste sludge to excellent N-CNT/AC composites for effective Cr(VI) removal.

4. Conclusion

A facile procedure of pyrolysis was proposed in this study in which industrial paper sludge was upgraded to biochar (BC-M) with N-doped carbon nanotubes/activated carbon composites in the presence of melamine. The carbon nanotubes with 50 nm diameter in-situ developed on biochar. This unique synthesized N-CNT/AC composites provided extraordinary electrochemical properties and sufficient reactive sites for Cr(VI) reduction, revealed by cyclic voltammetry, linear sweep voltammetry. Besides, the MEO/MER tests indicated that the BC-M displayed an excellent electron transfer potential compared with BC and pristine carbon electrode. Afterwards, enhanced Cr(VI) reduction was achieved in a traditional MFC configuration after simple surface fabrication of BC-M on graphite plate cathode, the Cr(VI) reduction efficiency increased to 55% compared with that of graphite electrode. This enhancement was attributed to superior electrochemical properties of BC-M. Such procedure for carbon nanotubes synthesis from sludge biomass has been rarely reported. The superior performance of biochar-derived carbon nanotubes/activated carbon composites could probably bring new thoughts on Carbon-neutral cycle and contaminants removal from a practical point in environmental remediation.

Declaration of competing interest

There are no conflicts of interests to declare.

Acknowledgements

This work was supported jointly by National Natural Science Foundation of China (No. 41877045, 21876032 and 21906028), Major Program of Higher Education of Guangdong (No. 2017KZDXM029) and Project funded by China Postdoctoral Science Foundation (No. 2019M652824).

Appendix A. Supplementary data

Supplementary data to this article can be found online at https://doi.org/10.1016/j.scitotenv.2020.136513.

References

Aeschbacher, M., Sander, M., Schwarzenbach, R.P., 2010. Novel electrochemical approach to assess the redox properties of humic substances. Environ. Sci. Technol. 44 (1), 87–93.

Bharath, G., Rambabu, K., Banat, F., Hai, A., Arangadi, A.F., Ponpandian, N., 2019. Enhanced electrochemical performances of peanut shell derived activated carbon and its Fe3O4 nanocomposites for capacitive deionization of Cr(VI) ions. Sci. Total Environ. 691, 713–726.

Bharath, G., Hai, A., Rambabu, K., Savariraj, D., Ibrahim, Y., Banat, F., 2020. The fabrication of activated carbon and metal-carbide 2D framework-based asymmetric electrodes for the capacitive deionization of Cr(VI) ions toward industrial wastewater remediation. Environ. Sci.: Water Res. Technol. https://doi.org/10.1039/C9EW00805E.

Bibi, I., Niazi, N.K., Choppala, G., Burton, E.D., 2018. Chromium(VI) removal by siderite (FeCO3) in anoxic aqueous solutions: an X-ray absorption spectroscopy investigation. Sci. Total Environ. 640, 1424–1431.

Chen, T., Zhou, Z.Y., Xu, S., Wang, H.T., Lu, W.J., 2015. Adsorption behavior comparison of trivalent and hexavalent chromium on biochar derived from municipal sludge. Bioresour. Technol. 190, 388–394.

Chen, X., Xu, J.Y., Chai, H., Wang, Y.C., Jia, D.Z., Zhou, W.Y., 2019. One-step synthesis of hollow chain-like nitrogen doped carbon nanotubes/iron carbide as highly efficient bifunctional oxygen electrocatalyst. J. Electroanal. Chem. 838, 16–22.

Gupta, S., Yadav, A., Verma, N., 2017. Simultaneous Cr(VI) reduction and bioelectricity generation using microbial fuel cell based on alumina-nickel nanoparticles-dispersed carbon nanofiber electrode. Chem. Eng. J. 307, 729–738.

Han, H.X., Shi, C., Zhang, N., Yuan, L., Sheng, G.P., 2018. Visible-light-enhanced Cr(VI) reduction at Pd-decorated silicon nanowire photocathode in photoelectrocatalytic microbial fuel cell. Sci. Total Environ. 639, 1512–1519.

Hsu, L., Masuda, S.A., Nealson, K.H., Pirbazari, M., 2012. Evaluation of microbial fuel cell Shewanella biocathodes for treatment of chromate contamination. RSC Adv. 2 (13), 5844–5855.

Kim, K., Choi, W., 2011. Enhanced redox conversion of chromate and arsenite in ice. Environ. Sci. Technol. 45 (6), 2202–2208.

Lei, E., Li, W., Ma, C.H., Xu, Z., Liu, S.X., 2018. CO2-activated porous self-templated N-doped carbon aerogel derived from banana for high-performance supercapacitors. Appl. Surf. Sci. 457, 477–486.

Li, M., Zhou, S.Q., 2019. Efficacy of Cu(II) as an electron-shuttle mediator for improved bioelectricity generation and Cr(VI) reduction in microbial fuel cells. Bioresour. Technol. 273, 122–129.

Li, H.X., Gong, Y., Fu, C.P., Zhou, H.H., Yang, W.J., Guo, M.L., Li, M.B., Kuang, Y.F., 2017. A novel method to prepare a nanotubes@mesoporous carbon composite material based on waste biomass and its electrochemical performance. J. Mater. Chem. A 5 (8), 3875–3887.

Li, M., Zhou, S.Q., Xu, Y.T., Liu, Z.J., Ma, F.Z., Zhi, L.L., Zhou, X., 2018. Simultaneous Cr(VI) reduction and bioelectricity generation in a dual chamber microbial fuel cell. Chem. Eng. J. 334, 1621–1629.

Li, Y.Y., Liang, J.L., Yang, Z.H., Wang, H., Liu, Y.S., 2019. Reduction and immobilization of hexavalent chromium in chromite ore processing residue using amorphous FeS2. Sci. Total Environ. 658, 315–323.

Liang, Q.H., Ye, L., Huang, Z.H., Xu, Q., Bai, Y., Kang, F.Y., Yang, Q.H., 2014. A honeycomb-like porous carbon derived from pomelo peel for use in high-performance supercapacitors. Nanoscale 6 (22), 13831–13837.

Pang, Y.M., Xie, D.H., Wu, B.G., Lv, Z.S., Zeng, X.H., Wei, C.H., Feng, C.H., 2013. Conductive polymer-mediated Cr(VI) reduction in a dual-chamber microbial fuel cell under neutral conditions. Synth. Met. 183, 57–62.

Qian, T., Wang, L., Le, C., Zhou, Y., 2019. Low-temperature-steam activation of phosphorus in biochar derived from enhanced biological phosphorus removal (EBPR) sludge. Water Res. 161, 202–210.

Sharma, P.P., Wu, J.J., Yadav, R.M., Liu, M.J., Wright, C.J., Tiwary, C.S., Yakobson, B.I., Lou, J., Ajayan, P.M., Zhou, X.D., 2015. Nitrogen-doped carbon nanotube arrays for high-efficiency electrochemical reduction of CO_2: on the understanding of defects, defect density, and selectivity. Angew. Chem.-Int. Edit. 54 (46), 13701–13705.

Tandukar, M., Huber, S.J., Onodera, T., Pavlostathis, S.G., 2009. Biological chromium(VI) reduction in the cathode of a microbial fuel cell. Environ. Sci. Technol. 43 (21), 8159–8165.

Tao, S.Y., Yang, J.K., Hou, H.J., Liang, S., Xiao, K.K., Qiu, J.J., Hu, J.P., Liu, B.C., Yu, W.B., Deng, H.L., 2019. Enhanced sludge dewatering via homogeneous and heterogeneous Fenton reactions initiated by Fe-rich biochar derived from sludge. Chem. Eng. J. 372, 966–977.

Wang, S.Z., Wang, J.L., 2019. Activation of peroxymonosulfate by sludge-derived biochar for the degradation of triclosan in water and wastewater. Chem. Eng. J. 356, 350–358.

Wang, Q., Huang, L.P., Pan, Y.Z., Quan, X., Puma, G.L., 2017. Impact of Fe(III) as an effective electron-shuttle mediator for enhanced Cr(VI) reduction in microbial fuel cells: reduction of diffusional resistances and cathode overpotentials. J. Hazard. Mater. 321, 896–906.

Wang, R.Z., Huang, D.L., Liu, Y.G., Zhang, C., Lai, C., Wang, X., Zeng, G.M., Gong, X.M., Duan, A., Zhang, Q., Xu, P., 2019. Recent advances in biochar-based catalysts: properties, applications and mechanisms for pollution remediation. Chem. Eng. J. 371, 380–403.

Xafenias, N., Zhang, Y., Banks, C.J., 2013. Enhanced performance of hexavalent chromium reducing cathodes in the presence of Shewanella oneidensis MR-1 and lactate. Environ. Sci. Technol. 47 (9), 4512–4520.

Yuan, Y., Bolan, N., Prevoteau, A., Vithanage, M., Biswas, J.K., Ok, Y.S., Wang, H.L., 2017. Applications of biochar in redox-mediated reactions. Bioresour. Technol. 246, 271–281.

Zhang, Y.F., Angelidaki, I., 2014. Microbial electrolysis cells turning to be versatile technology: recent advances and future challenges. Water Res. 56, 11–25.

Zhang, B., Zhou, S., Zhou, L., Wen, J., Yuan, Y., 2019a. Pyrolysis temperature-dependent electron transfer capacities of dissolved organic matters derived from wheat straw biochar. Sci. Total Environ. 696, 133895.

Zhang, Q., Song, Y.Z., Amor, K., Huang, W.E., Porcelli, D., Thompson, I., 2019b. Monitoring Cr toxicity and remediation processes - combining a whole-cell bioreporter and Cr isotope techniques. Water Res. 153, 295–303.

Zhang, T., Hu, L., Zhang, M., Jiang, M., Fiedler, H., Bai, W., Wang, X., Zhang, D., Li, Z., 2019c. Cr(VI) removal from soils and groundwater using an integrated adsorption and microbial fuel cell (A-MFC) technology. Environmental Pollution (Barking, Essex : 1987) 252 (Pt B), 1399–1405.

Zhang, X.Q., Xia, J., Pu, J.Y., Cai, C., Tyson, G.W., Yuan, Z.G., Hu, S.H., 2019d. Biochar-mediated anaerobic oxidation of methane. Environ. Sci. Technol. 53 (12), 6660–6668.

Zhong, D., Jiang, Y., Zhao, Z., Wang, L., Chen, J., Ren, S., Liu, Z., Zhang, Y., Tsang, D.C., Crittenden, J.C., 2019. pH dependence of arsenic oxidation by rice-husk-derived biochar: roles of redox-active moieties. Environ. Sci. Technol. 53, 9034–9044. https://doi.org/10.1021/acs.est.9b00756.

Zhou, L.H., Fu, P., Wang, Y.Q., Sun, L.H., Yuan, Y., 2016. Microbe-engaged synthesis of carbon dot-decorated reduced graphene oxide as high-performance oxygen reduction catalysts. J. Mater. Chem. A 4 (19), 7222–7229.

Zhou, L.H., Yang, C.L., Wen, J., Fu, P., Zhang, Y.P., Sun, J., Wang, H.Q., Yuan, Y., 2017. Soft-template assisted synthesis of Fe/N-doped hollow carbon nanospheres as advanced electrocatalysts for the oxygen reduction reaction in microbial fuel cells. J. Mater. Chem. A 5 (36), 19343–19350.

Zhou, S., Huang, S., Li, X., Angelidaki, I., Zhang, Y., 2018a. Microbial electrolytic disinfection process for highly efficient Escherichia coli inactivation. Chem. Eng. J. 342, 220–227.

Zhou, S.F., Huang, S.B., Li, Y., Zhao, N.N., Li, H., Angelidaki, I., Zhang, Y.F., 2018b. Microbial fuel cell-based biosensor for toxic carbon monoxide monitoring. Talanta 186, 368–371.

Zhou, S.F., Zhou, L.H., Zhang, Y.P., Sun, J., Wen, J.L., Yuan, Y., 2019. Upgrading earth-abundant biomass into three-dimensional carbon materials for energy and environmental applications. J. Mater. Chem. A 7 (9), 4217–4229.